Transactions of the Materials Research Society of Japan 33[4] 893-896 (2008)

Structural and Magnetic Properties of Pt/Fe(111) Multilayered Films Containing Monolayer-thick Fe Layers

N. Nakayama, H. Tanabe, A. Satoh, Y. Mugita, A. Nakatsuka, S. Nagata[1] and Y. Ueda[2]
Graduate School of Science and Engineering, Yamaguchi University, Ube 755-8611,
[1]IMR, Tohoku University, Sendai, [2]ISSP, University of Tokyo, Kashiwa
Fax: 81-836-85-9601, e-mail: nakayamn@yamaguchi-u.ac.jp

The [111] oriented Pt/Fe multilayered films were fabricated by electron beam evaporation in an ultra-high vacuum of 10^{-8} Pa. Keeping the thickness of Fe at 0.2 nm corresponding to one atomic monolayer (ML), several samples with the different Pt layer thickness (n_{Pt}) from 1 to 8 ML were deposited on the Si-wafer covered with 20 nm thick Au(111) buffer layer. XRD patterns of the samples with $n_{Pt} \geq 2$ showed well-resolved superlattice peaks. Superlattie periods from XRD and atomic compositions evaluated by RBS spectra almost agree with the designed ones. All the films are ferromagnetic even at room temperature. The magnetization decreases with the increase of n_{Pt} at 300 K, suggesting the two dimensional effect for high n_{Pt}. For the sample with n_{Pt} =8, the perpendicular magnetic anisotropy was observed at 5 K. Details of the XRD intensity analysis indicate the alloy layer formation.
Key words: superlattice films, interface alloying, magnetic anisotropy, XRD, RBS

1. INTRODUCTION

Thin films of Fe-Pt alloys have long received much attention because of their potential ability for the magnetic recording applications. In last decades, [100] oriented Fe/Pt multilayered films have been extensively investigated. [1-4] Many of them aim to fabricate [100] oriented and $L1_0$-type ordered PtFe[100] thin films. The [111] oriented films are also interesting in the viewpoints of the magnetic anisotropy and the induced magnetic moment of Pt layers [5,6].

The $L1_0$-type structure can be assumed as the stacking of fcc-(001) Fe and Pt monolayer. The Fe/Pt multilayered films with fcc-[001] orientation have been extensively investigated in this decade in this context. Shima et al. have succeeded in the fabrication of single crystalline $L1_0$-FePt thin films by depositing the atomic thick Fe and Pt alternately on MgO[001] substrate kept at the relatively low temperature about 230 °C.[4] Although their films show perpendicular magnetic anisotropy, the coercive force is not enough to use as recording media.

The [111] oriented Fe/Pt multilayered films have also investigated to obtain the $L1_0$-PtFe films by annealing the multilayered films [7]. The rapid annealing at relatively high temperature, around 500 °C, seems to be effective to obtain the PtFe alloy films with perpendicular magnetic anisotropy. However, the structure and the reactivity of ultra-thin Fe(111) layers in the multilayered films have not fully been investigated.

Recently, atomic thick Fe layers deposited on Pt(111) or Pt(997) substrate have been investigated by several authors [8,9] using the surface characterization methods; LEED, XPS, and/or SMOKE. According to their results, Fe grows pseudo-morphologically on Pt(111) and Pt(997) substrates at room temperature in the thickness range from sub-one to two monolayer. With incasing the thickness over 3 monolayer (ML), the 3-dimesional growth takes place. At the substrate temperature, around 200 °C, the alloy layers are formed. These results suggest the stability of monolayer-thick Fe(111) layers in the Pt/Fe multilayered films.

In this paper, we describe structural and magnetic properties of [111] oriented Pt/Fe mutilayered films in which nominally designed Fe layer thicknesses are 0.2 nm, which corresponds to one atomic monolayer (1 ML). Several samples with different Pt layer thicknesses ($1 \leq n_{Pt} \leq 8$ ML) were prepared by a vacuum evaporation method and the variation of structural and magnetic properties with n_{Pt} has been investigated.

2. EXPERIMENTAL

Films were deposited in an ultra-high vacuum of 10^{-8} Pa order by using an electron beam evaporation system. The film thickness was measured during deposition by using quartz thickness monitors (Inficon XTC2 and XTM). The substrates were glass-plate and Si-wafer without surface cleaning in the vacuum chamber. At first, a 20 nm-thick Au(111) or 25 nm-thick Pt(111) buffer layers were deposited with keeping the substrate temperature at room temperature. After the deposition, these buffer layers were annealed at 200 °C for several hours to get the flat surfaces. The RHEED patterns were used to check the film orientation and the surface quality. In the film plane, the buffer layers are composed of randomly oriented grains with average diameter of a few micrometers. After the substrate temperature was reduced to be ambient temperatures, Fe/Pt multilayered films were deposited.

The film compositions were analyzed by RBS methods. The RBS spectra of samples deposited on Si substrate were obtained using 2MeV $4He^{2+}$ ions from a tandem accelerator at Institute for Material Research,

Tohoku University. To evaluate the atomic area densities, the profile fitting was performed using a computer code described elsewhere [10]. The x-ray diffraction patterns were measured to investigate the film structures by using a powder diffractometer (Rigaku-RAD-B) with a thin film attachment. The Cu-Kα radiation form a rotating anode type x-ray generator (RIGAKU RU-200) was used for the measurements. The simulation and the profile fitting of x-ray diffraction patterns were performed by using a computer program ASFHT [11]. For the magnetization measurements, a vibrating sample magnetometer was used at room temperature. A SQUID magnetometer was used for the measurements at low temperatures.

3. RESULTS and DISCUSSION

3.1 X-ray diffraction patterns

Figure 1 shows x-ray diffraction patterns of [Fe(1ML)/Pt(nML)]$_{40}$/Au(20nm)/Si(100) multilayered films (n = 1, 2, 5, 8), observed in the θ–2θ geometry with the scattering vector perpendicular to the film planes. The diffraction patterns show intense peaks of fcc 111 reflection from multilayered films together with intense 111 peak of Au. A weak 200 reflection from the mis-oriented Au grains in the buffer layers is seen for the samples with n=1 and 2. Other peaks marked by filled circles are superlattice reflections from multilayered films. The superlattice periods for samples with Pt layer thickness larger than n = 2 well agree with the sum of designed thickness of Fe and Pt layers. The thicknesses of one atomic layer (1ML) of Fe and Pt were designed as 2.07 and 2.26 Å, respectively. The designed periods are 6.6, 13.4, and 20.2 Å for n = 2, 5, and 8, respectively. The observed periods are 6.8, 14.3, and 21.8 Å, respectively. No superlattice reflection was observed for [Fe(1ML)/Pt(1ML)] multilayers, suggesting the interface roughness within a few atomic layers.

The d-values of fundamental 111 reflections of Fe/Pt multilayers increase with increasing Pt layer thickness as shown in Fig.2. If the (111) lattice spacings in the Pt layers are uniform (d_{Pt}), the average lattice spacing <d> is given by following equation, where d_{Fe} is the thickness of Fe atomic layer.

$$< d >_{111} = (nd_{Pt} + d_{Fe})/(n+1) \qquad (1)$$

The line plot in Fig.2 shows calculated <d> using Eq. 1 and the (111) lattice spacing of bulk fcc-Pt (d_{Pt} = 2.26 Å) and fcc-Fe (d_{Fe} = 2.07 Å). The observed <d> values are larger than the calculated ones and can be reproduced assuming as d_{Pt} = 2.247 Å and d_{Fe} = 2.139 Å. The <d> value of the sample with n = 1 (2.19 Å) is close to the (111) lattice spacing (2.20 Å) of disordered Fe50Pt50 alloy, suggesting the some mixing of Fe and Pt atoms at the interfaces.

3.2 RBS spectra

Figure 2 shows typical 2 MeV He^{2+} RBS spectra of [Fe(1ML)/Pt(nML)]$_{40}$/Au(20nm) (n=1,5) multilayered films and the results of profile fitting to evaluate the atomic area densities. To avoid the channeling effect of Si substrate, the incident beam was tilted to 7 °. The detector angle is 170 °. The beam size is 1.3 mm and the

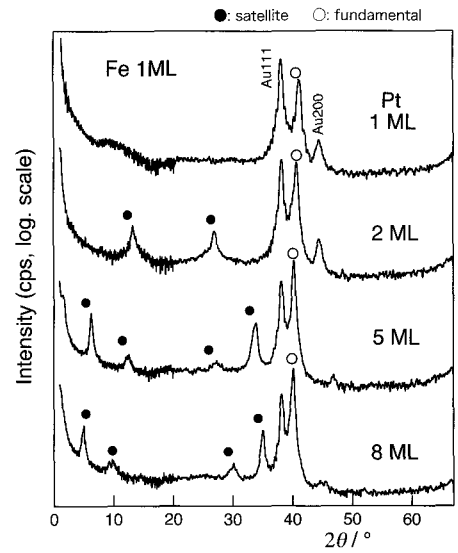

Fig.1 X-ray diffraction patterns (θ–2θ scan) of [Fe(1 ML)/Pt(n ML)]40/Au(20 nm) multilayered films deposited on Si substrate.

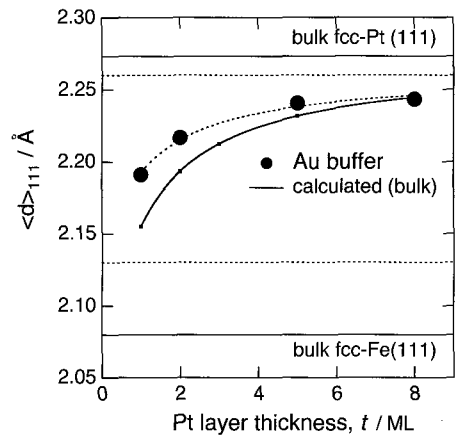

Fig.2 Observed and calculated average fcc (111) lattice spacing <d> of [Fe(1 ML)/Pt(n ML)]$_{40}$ multilayers.

beam current was typically 2 nA. The atomic area densities of Pt, Fe and Au almost agree with the designed thicknesses. The area densities expected for the designed thickness are shown in Fig. 3 as dashed lines. Some discrepancies may be ascribed to the systematic errors in the profile fitting, because the backscattering peaks of Au and Pt are overlapped. The slight tailing on the low energy side of Au peak and the higher energy side of Si edge suggest some intermixing at the Au/Si interfaces caused by the annealing at 200 °C.

3.3 Magnetization

Figure 4(a) shows magnetization curves at room temperature. All the films show ferromagnetic hysteresis loops but some Pt thickness dependences were observed. With increasing Pt layer thickness or the number of Pt atomic layers (n), the magnetization at H = 10000 Oe decreases. The loops for n = 1 and 2 show rectangular

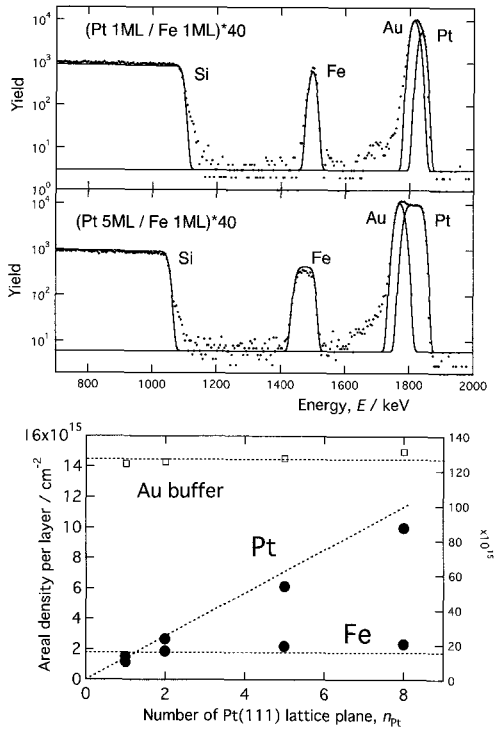

Fig.3 Typical 2 MeV He^{2+} RBS spectra of [Fe(1 ML)/Pt(n ML)]$_{40}$ multilayers (n = 1, 5) and the results of profile fitting to evaluate the atomic area densities.

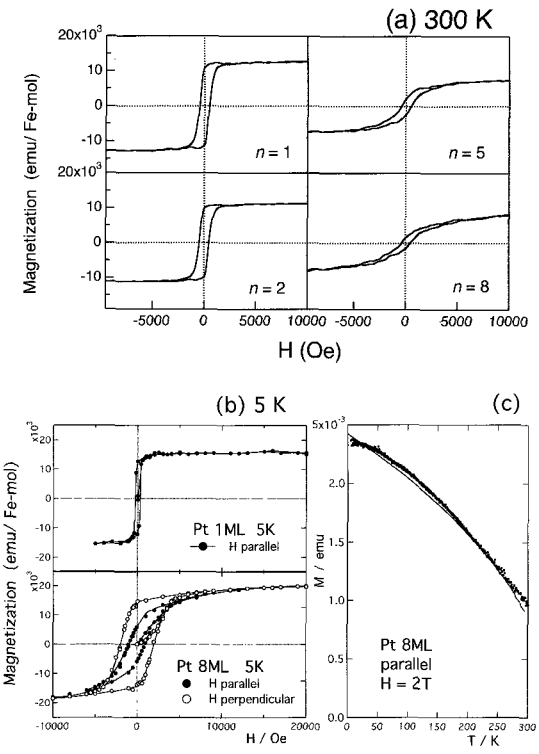

Fig.4 Magnetization curves at room temperature (a) and 5 K (b) for [Fe(1 ML)/Pt(n ML)]$_{40}$ multilayers. The temperature dependence of magnetization for a sample with 8 ML-thick Pt layers is shown in (c).

shapes, whereas those for n = 5 and 8 do not show saturation even at H = 10000Oe. Magnetically easy directions were in the film plane for all the samples. These results suggest two-dimensional magnetic behavior for the samples with n = 5 and 8.

Figure 4(b) shows magnetization curves at 5 K for the samples with n = 1 and 8. The curve for n = 1 shows about 20% increase of saturation magnetization from the room temperature value but the coercive force is not so much changed (300 Oe). The magnetically easy direction is in the film plane. On the other hand, the sample with n = 8 shows the enhancement of magnetization more than twice of the room temperature value at H = 10000 Oe. The saturation magnetization corresponds to about 3 μ_B per Fe atoms, if the induced magnetization of Pt is ignored. The coercive force also increases to be more than 1000 Oe and the perpendicular direction to the film plane turns to be more easily magnetized. Figure 4(c) shows the temperature dependence of magnetization for the sample with n = 8. The applied magnetic field was 2 T in the in-plane direction. The magnetization steeply decreases with increasing temperature. Such a steep decrease suggests the two dimensional effect. The rough estimation of Curie temperature, T_c, by applying a phenomenological formula (Eq.2), gives a value of 400 K.

$$M/M_S = (1-T/T_c)^{\beta} \qquad (2)$$

The above magnetic behavior suggests that Fe layers in the present samples are close to the disordered PtFe alloys, of which Cuire temperature is 600K for Fe50Pt50 and magnetic moment is 2.8 μ_B per Fe atom [12]. In the case of the sample with n = 8, the separation of Fe layers by Pt layers may induce the two dimensional behavior. The magnetic behavior for the sample with n = 1 can be interpreted as a three dimensional one because of the interface roughness or interdiffusion.

3.4 Simulation of x-ray diffraction profiles

The magnetic properties of the present samples with monolayer-thick Fe layers suggest the alloy layer formation due to the interface roughness. The observed x-ray diffraction patterns were compared with the simulated ones assuming the alloy layer formation. The x-ray diffraction profiles were simulated based on the step model [13] as described by Eq. (3), f, σ, Q, and Λ are x-ray atomic scattering factor, plane density, scattering vector, and superlattice period, respectively.

$$|F(Q)|^2 = f_{Pt}^2\sigma_{Pt}^2\frac{\sin^2(n_{Pt}Qd_{Pt}/2)}{\sin^2(Qd_{Pt}/2)} + f_{Fe}^2\sigma_{Fe}^2\frac{\sin^2(n_{Fe}Qd_{Fe}/2)}{\sin^2(Qd_{Fe}/2)} + f_{Pt}f_{Fe}\sigma_{Pt}\sigma_{Fe}\frac{\sin(n_{Pt}Qd_{Pt}/2)}{\sin(Qd_{Pt}/2)}\frac{\sin(n_{Fe}Qd_{Fe}/2)}{\sin(Qd_{Fe}/2)}\cos(\Lambda Q/2) \qquad (3)$$

Figure 5(a) shows those for ideal Pt/Fe superlattices. The atomic layer thicknesses are d_{Pt} = 2.263 Å and d_{Fe} = 2.148 Å, which agree with the observed average lattice spacing <d> shown in Fig. 2. The plane densities are set to be identical. Figure 5(b) shows those assuming alloy layer formation with the composition of Fe50Pt50 (d_{FePt} = 2.184 Å). Under this assumption, the nominal

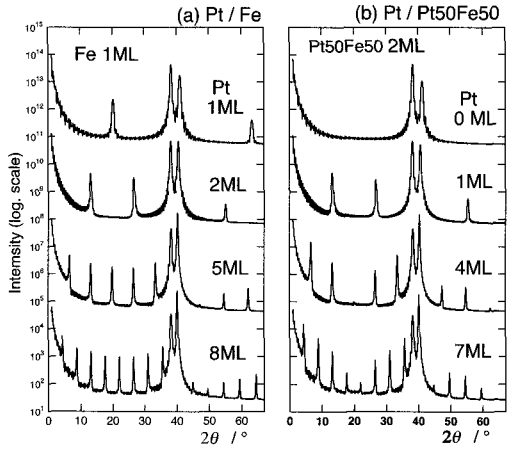

Fig.5 Calculated XRD profiles based on the step model for (a) [Fe(1 ML)/Pt(n ML)]$_{40}$ and (b) [FePt(2 ML)/Pt(n − 1 ML)]$_{40}$ multilayers.

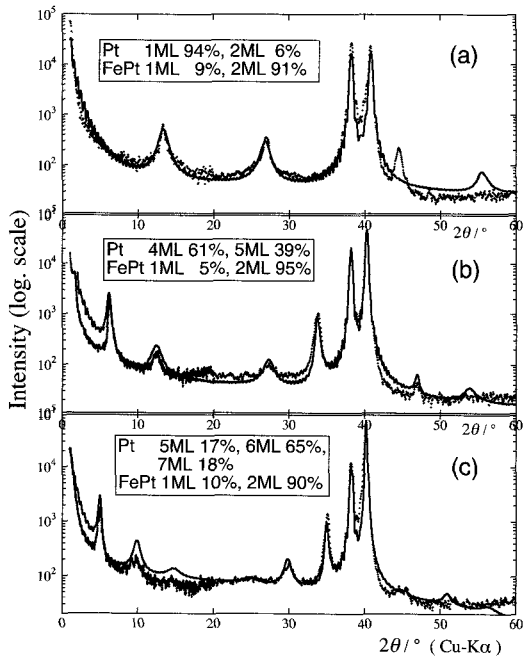

Fig.6 Calculated XRD profiles for [FePt(2 ML)/Pt(n-1 ML)]$_{40}$ multilayers based on the HT model taking the layer thickness fluctuation into account. Observed profiles are shown as dot plots. The nominal Pt thicknesses are 2 ML (a), 5 ML (b) and 8 ML (c), respectively.

atomic Fe monolayers turn into two-monolayer-thick PtFe alloy layers and the number of Pt atomic layer reduced by one. XRD patterns in Fig. 5(b) show the decrease in the intensity of higher order superlattice reflections, as is seen for the observed profiles. However, the observed intensities do not so well agree with those in Fig. 5(b).

To reproduce the observed intensity, some layer thickness fluctuation should be assumed. The interface roughness to form the alloy layer may cause the layer thickness fluctuations in the range one or two monolayer thickness. The diffraction profiles were simulated using Hendrixs and Teller formula [11,14,15] as shown in Fig. 6. The d-values are the same to those for Fig. 5(b). The probabilities of PtFe alloy layers and pure Pt layers with different thickness are shown in Fig. 6. With these values observed profiles are qualitatively reproduced.

4. SUMMARY

Fcc [111] oriented Pt/Fe multilayered films with the monolayer thick Fe layers have been successfully fabricated. Observed XRD patterns are well reproduced by assuming the formation of alloy layers with some layer thickness fluctuation. The ferromagnetic behavior of the present samples also agrees with the alloy layer formation. When Pt layers are enough thick, a two-dimensionality of alloy layer affects on the temperature dependence of magnetization. The contribution of induced magnetic moments in the Pt layer is interesting to interpret the Pt layer thickness dependence of magnetic properties.

ACKNOWLEDGEMENTS

The RBS study in this work was performed under the cooperative research programs of IMR, Tohoku University. Also the authors thank the Materials Design and Characterization Laboratory, Institute for Solid State Physics, University of Tokyo for the facilities.

REFERENCES

[1] M. Sakurai, *Phys. Rev.*, **B50**, 3761 (1994) , *J. Appl. Phys.*, **76**, 7272 (1994).
[2] T. C. Hufnagel, M. C. Kautzky, B. J. Daniels, and B. M. Clemens, *J. Appl. Phys.*, **85**, 2609 (1999).
[3] W. J. Antel, Jr., M. M. Schwickert, and Tao Lin, W. L. O'Brien, and G. R. Harp, *Phys. Rev.*, **B60**, 12933 (1999).
[4] T. Shima, T. Moriguchi, S. Mitani, and K. Takanashi, *Appl. Phys. Lett.*, **80**, 288 (2002)
[5] A. Simopoulis, E. Devlin, A. Kostikas, A. Jankowski, M. Croft, and T. Tsakalakos, *Phys. Rev.*, **B 54**, 9931 (1996).
[6] S. Yamamoto, T. Kato, S. Iwata, and S. Tsunashima, S. Uchiyama, *J. Appl. Phys.*, **95**, 7285 (2004).
[7] H. Zeng, M. L. Yan, N. Powers, and D. J. Sellmyer, *Appl. Phys. Lett.*, **80**, 2350 (2002).
[8] R. Cheng, K. Yu. Guslienko, F. Y. Fradin, J. E. Pearson, H. F. Ding, Dongqi Li, and S. D. Bader, *Phys. Rev.*, **B72**, 014409 (2005).
[9] Y.J. Chen, H.Y. Ho, C.C. Tseng, and C.S. Shern, *Surf. Sci.*, **601**, 4334 (2007).
[10] Y. Tsuchiya, K. Kosuge, S. Yamaguchi, and N. Nakayama, *Materials Trans. JIM*, **38**, 91 (1997).
[11] N. Nakayama, T. Okuyama, and T. Shinjo, *J. Phys. Condens. Matter*, **5**, 1173 (1993).
[12] A. Kussmann and G. Rittberg, Ann. Phys., **7** 173 (1950); J. Crangle, *J. Phys. Paris*, **20**, 435 (1959).
[13] Y. Fujii, T. Ohnishi, T. Ishihara, Y. Yamada, K. Kawaguchi, N. Nakayama, and T. Shinjo, *J. Phys. Soc. Jpn.*, **55**, 251 (1986).
[14] S. Hendricks and E. Teller, *J. Chem. Phys.*, **10**, 147 (1942).
[15] E. E. Fullerton, I. K. Schuller, H. Vanderstraeten and Y. Bruynseraede, *Phys. Rev.*, **B45**, 9292 (1992).

(Recieved December 28, 2007; Accepted May 2, 2008)